Gas Transport Properties of Poly(trimethylsilylpropyne) and Ethylcellulose Filled with Different Molecular Weight Trimethylsilylsaccharides: Impact on Fractional Free Volume and Chain Mobility

J. Qiu,[†] J.-M. Zheng,[‡] and K.-V. Peinemann*,[†]

Institute of Polymer Research, GKSS Research Centre Geesthacht GmbH, Max-Planck-Strasse 1, D-21502 Geesthacht, Germany, and LEPAE, Chemical Engineering Department, Faculty of Engineering, University of Porto Rua Dr. Roberto Frias, 4200-465 Porto, Portugal

Received July 1, 2006; Revised Manuscript Received January 15, 2007

ABSTRACT: This work aims to systematically investigate the gas transport behavior in two glassy polymers. One is the rigid, high fractional free volume (FFV) poly(1-trimethylsilyl-1-propyne) [PTMSP], and the other is the relatively flexible, considerably lower FFV ethylcellulose (EC). Both polymer systems are filled with a series of various molecular weight (M_w) trimethylsilylsaccharides [TMSS] (trimethylsilylglucose (M_w = 180) [TMSG], trimethylsilyldextran1 (M_w = 900−1200) [TMSD1], and trimethylsilyldextran500 (M_w = 350K−550K) [TMSD500]). The consistent trend of decreasing gas permeability, diffusivity, and solubility with increasing load of the TMSS fillers was observed in the PTMSP/TMSS system. In addition, the extent of reduction of gas permeability, diffusivity, and solubility in these composites is closely related to the M_w of TMSS fillers at an equivalent load of various TMSS in the PTMSP matrix. For example, the PTMSP permeability to nitrogen reduced 227-fold, 43-fold, and 4-fold when filled with constant 27.2% TMSG, TMSD1, and TMSD500, respectively. The diffusivity decreased 45-fold, 21-fold, and 3-fold, and the solubility decreased 5.0-fold, 2.0-fold, and 1.3-fold, respectively. The decreases in permeability, diffusivity, and solubility are directly related to the decrease of FFV in PTMSP caused by the incorporation of the various M_w fillers. In contrast to the decrease of permeability observed in the PTMSP/TMSS system, a systematic increase of gas permeability and diffusivity was obtained for the EC/TMSS system with increasing load of TMSS fillers. However, no consistent change of solubility was observed in EC/TMSS. Moreover, the gas diffusivity increase for the EC/TMSS system correlated well with the M_w of the TMSS fillers, in contrast to the permeability increase. For example, when TMSG, TMSD1, and TMSD500 were used as fillers, the permeability to nitrogen of EC composites with 32.1% fillers increased 1.75-fold, 1.81-fold, and 1.64-fold, respectively, compared to that in unfilled EC. The diffusivity increased 3.32-fold, 1.84-fold, and 1.31-fold, and the solubility increased −1.87-fold, 0-fold, and 1.25-fold, respectively. All applied TMSS fillers led to an increase of gas diffusivity, which can be attributed to an increased chain mobility. The chain mobility changes in EC/TMSS resulted in changes of the excess FFV of EC and therefore altered the gas solubility. The increase extent of chain mobility was the highest with the lowest M_w TMSS.

Introduction

Gas transport through dense polymer film is based on the well-known solution−diffusion mechanism.[1] The sorption for a nonpolar gas is primarily related to gas condensability and polymer fractional free volume (FFV).[2,3] It should be noted that the "excess FFV" is commonly present in glassy polymers but not in rubbers because the restricted polymer segmental mobility in the glassy state leads to a surplus in FFV compared to that in the equilibrium state.[4] Consequently, the gas solubility in glassy polymers is generally higher than that in thermodynamic equilibrium rubbery polymers due to the excess FFV.[5] Another term, i.e., gas diffusion, is mainly related to the effective gas molecule size and polymer's FFV as well as to the polymer chain mobility.[2,3] Cohen et al.[6] have developed a mathematic correlation between gas diffusivity and the inverse of the FFV. However, the direct correlation between gas diffusivity and polymer chain mobility is less reported. But, the approaches of estimation of gas permeability using the combination of FFV and cohesive energy density were evaluated by Jia and Xu,[7] Thran et al.,[8] and Nagel et al.[9]

The designing of new gas separation materials should predominantly focus on modifying polymer chain packing (i.e., FFV) and mobility. It is worthwhile to mention two representative polymers. One is the highest permeable polymer poly(1-trimethylsilyl-1-propyne) [PTMSP] with the unusually large FFV (0.29), which results from the rigid −C═C− backbone containing the bulky trimethylsilyl pending group.[10,11] Prior to the invention of PTMSP, rubbery polydimethylsiloxane [PDMS] was the highest permeable polymer due to the high flexibility of the siloxane (−Si−O−) linkages in this polymer.[12] It is clear that an extremely high FFV or high mobility leads to a fast permeability but also to a low size selectivity. Recently, polymers of intrinsic microporosity (PIM) were discovered to have rigid but contorted molecular structures, which frustrated packing and created high FFV. This significantly improved permeability and size selectivity performances.[13] Such polymers are in agreement with Petropoulos's and Freeman's proposal;[2,14] i.e., the chain stiffness and the properly enhanced interchain space will break Robeson's tradeoff line.[15] Moreover, Lin and Freeman[16] discovered that the increased chain mobility in the highly cross-linked poly(ethylene oxide) by plasticization can lead to a distinguished separation performance for the large gas

* Corresponding author: Tel +0049-4152-872420; Fax +0049-4152-872466; e-mail klaus-viktor.peinemann@gkss.de.
[†] GKSS Research Centre Geesthacht GmbH.
[‡] University of Porto Rua Dr. Roberto Frias.

10.1021/ma0614794 CCC: $37.00
Published on Web 03/30/2007

Table 1. Physical Properties of Trimethylsilylsaccharides (TMSS) Fillers

name	trimethylsilyl -glucose	trimethylsilyl –dextran1	trimethylsilyl -dextran500
acronym	TMSG	TMSD1	TMSD500
structure [a]		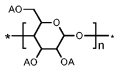	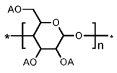
molecular weight [b]	180	900-1200	350-550k
silylation degree %	83	80	78
T_g (°C)	-	69.5	128.4-136.5
onset of weight loss (°C)	110	240	-
density (g/cm^3) [c]	0.98 ± 0.15	0.97 ± 0.2	0.96 ± 0.2

[a] A = −H or −Si(CH$_3$)$_3$. [b] Molecular weight is based on the saccharides without silyl group. [c] The density of polymers is determined from their weight and volume at room temperature.

CO_2 over the small gas H_2 (so-called the reverse selectivity). This work may suggest that the polymer chain mobility is likely to be a key factor to improve the reverse selectivity in membranes.

Compared to the synthesis of new materials with high cost and considerable time, modifying existing polymer materials is a feasible strategy to obtain improved separation performance. For example, nonporous, nanosized inorganic particles like silica have been added to the super glassy polyacetylene polymer matrix, resulting in increased FFV and consequently an increased permeability and permselectivity of condensable gas/noncondensable gas (e.g., butane/methane).[17] Polyacetylenes filled with very small inorganic fillers such as fullerene[18] and small size organic additives[19,20] result in a decreased FFV accompanied by increased size selectivity. In addition, PTMSP with large size of organic fillers such as PDMS,[21] poly(4-methyl-2-pentyne) [PMP],[22] poly(*tert*-butylacetylene) [PTBA],[22] and poly(1-phenyl-1-propyne) [PPP][23] lead to the decreased permeability with increased permselectivity. In our latest study of the PTMSP/TMSG composite,[20] the adjustable addition of TMSG filler is a facile method to tailor the permeability/selectivity performance of high free volume PTMSP.

Moreover, the size of the fillers seems to be closely related to the permeability change. For example, Merkel et al.[17] found out that the permeability increases in the polyacetylene (PMP) with the incorporation of eight different size particles (primary particle diameter 7−500 nm) with different surface chemistries. Recently, Andrady et al.[24] incorporated silica (primary particle size: 7−40 nm) modified with hexamethyldisilazane or dimethyldichlorosilane into the rigid PTMSP. They also found a pronounced correlation between relative permeability and primary particle diameter of the filler. In contrast, a decreased permeability was observed in the flexible PDMS loaded with decreasing zeolite particle size.[25]

In addition to the filler-size-related permeability change, the rigidities of the filler and the polymer matrix also have an influence on the transport properties of the filled system. To our knowledge, all flexible organic fillers in PTMSP led to a decreased permeability compared to pure PTMSP. In contrast, rigid inorganic fillers such as fumed silicas in PTMSP increased the permeability. The rigidity of the polymer is indicated by opposite permeability changes for flexible PDMS[25] and rigid PTMSP[24] filled with rigid particles, i.e., zeolites and fumed silica.

In this study, we extend our previous work[20] to fill the high FFV and rigid PTMSP with a series of trimethylsilylsaccharides (i.e., trimethylsilyldextran1 [TMSD1] (M_w = 900−1200) and trimethylsilyldextran500 [TMSD500] (M_w = 350K−550K)) with larger molecular weight relative to the TMSG (M_w = 180) analogue. Besides, three TMSS fillers have also been added to the low FFV, more flexible EC for comparison. The impact of various M_w of TMSS fillers in two different polymer matrices on the free volume and chain mobility is comprehensively discussed and associated with the gas transport properties.

Table 2. Physical Properties of Ethylcellulose and Poly(1-trimethysilyl-1-propyne)

polymer	ethylcellulose	poly(1-trimethysilyl-1-propyne)
acronym	EC	PTMSP
structure	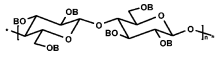	
molecular weight	-	480 kDa [20]
T_g (°C)	125 - 130	> 250 [26]
density (g/cm^3) [a]	1.12±0.02	0.78±0.02
fractional free volume	0.15	0.30
ethoxy content	46 %	-

[a] The density of polymers is determined from their weight and volume at room temperature.

Experimental Section

Synthesis and Characterization of Trimethylsilylsaccharides (TMSS). Dextran1 and dextran500 were obtained from Aldrich. The silylation of TMSD1 and TMSD500 has been likewise described in our previous article.[20] The silylated products were characterized by proton nuclear magnetic resonance (^{1}H NMR) and thermogravimetry analysis (TGA). The overall silylation degree was 80% for TMSD1 and 78% for TMSD500 with a good reproducibility, based on ^{1}H NMR spectra. The thermal stability determined by TGA, the glass transition temperature determined by DSC, and the density of TMSS are presented in Table 1.

PTMSP/TMSS and EC/TMSS Composites Film Preparation and Characterization. PTMSP and EC were purchased from Gelest (Lot: 5I-7401) and Aldrich, respectively. The following physical properties for both polymers are presented in Table 2: the molecular weight, density, fractional free volume, and glass-transition temperature. The preparation of 1% (w/v) PTMSP/TMSS composites is described elsewhere. For the EC/TMSS composites system, a relatively higher concentration of EC polymer solution (i.e., 2% (w/v)) in dry chloroform was prepared. The casting film procedure followed the script in the PTMSP/TMSS system. Film thickness in the PTMSP/TMSS and EC/TMSS composites varied from 120 to 250 μm and from 50 to 120 μm, respectively, which was measured by a digital micrometer with a precision of ±2 μm. Finally, the films were cut into round disks with diameter of 4.6 cm for a time-lag test cell. The freshly prepared PTMSP/TMSS films were directly analyzed by the time-lag method in order to reduce the influence of PTMSP aging as much as possible. EC/TMSS films are storable.

(a) Differential Scanning Calorimeter. Thermal analysis for EC/TMSS (32 vol %) composites was carried out using a differential scanning calorimeter (DSC) (Netzsch Thermal Analysis DSC204, Germany). The glass transition temperatures for PTMSP/TMSS system are absent because the polymer PTMSP does not exhibit a clear T_g.[26] Before the analysis, the samples were dried in a vacuum oven at 80 °C overnight. DSC scans were performed under a nitrogen atmosphere at a heating rate of 10 °C/min from −50 to 110 °C for the first scan and then cooling to −50 °C at the same rate. The second scan was heated from −50 to 150 °C for determination of glass transition temperature. To determine the crystallinity of EC, the unfilled EC was heated from RT to 300 °C and cooling from 300 °C to RT at a rate of 10 °C/min, no crystallization endotherm and exotherm have been observed.

(b) Scanning Electron Microscopy (SEM). Scanning electron microscopy was performed to investigate the morphology of EC/TMSS and PTMSP/TMSS composites with a LEO 1550 VP Gemini from ZEISS instrument. The specimens were frozen under liquid nitrogen, as described elsewhere,[27] then fractured, mounted, and coated with 2 nm Au/Pd in a magnetron sputtering process (Emitec K575). SEM cross-section micrographs were obtained at 1 and 3 kV accelerating voltage for ethylcellulose and PTMSP composites,

respectively. The low accelerating voltage was chosen for the electron beam sensitive saccharides.

(c) Gas Transport Properties. Gas permeation data were measured at 30 °C with six pure gases (helium, hydrogen, carbon dioxide, oxygen, nitrogen, and methane) with a pressure increase time-lag apparatus, which has been described elsewhere.[28] The feed pressure used was between 200 and 400 mbar for the larger gases (carbon dioxide, oxygen, nitrogen, and methane) and around 100 mbar for smaller gases (helium and hydrogen). The permeate pressure was maintained at less than 10^{-7} bar with an oil-free vacuum pump. The gas permeability P was calculated under steady state (constant permeance) by eq 1:

$$P = \frac{V_p l}{ART\Delta t} \ln\left(\frac{p_f - p_{p_1}}{p_f - p_{p_2}}\right) \quad (1)$$

where V_p is the constant permeate volume (m^3), l is the film thickness (m), R is the gas constant (8.314 Pa m^3 mol^{-1} K^{-1}), A is the film area (m^2), T is the temperature (K), Δt is the time (s) for permeate pressure increase from p_{p_1} to p_{p_2}, p_f is feed pressure (Pa), and the unit of P is mol m^{-1} s^{-1} Pa^{-1}. To obtain the permeability in barrer (10^{-10} cm^3 (STP) cm/(cm^2 s cmHg), the value has to be multiplied by 2.99×10^{15}.

The solution−diffusion transport model is applied for gas transport process through dense polymer film. It means that the permeability coefficient P can be defined as

$$P = DS \quad (2)$$

where D is the steady diffusion coefficient (cm^2/s) and S is the solution coefficient (cm^3 (STP)/(cm^3 cmHg)). The diffusion coefficient D can be directly obtained by the time-lag method under the assumption of a constant diffusion coefficient. As the gas transport through the film reaches a steady state, the diffusion coefficient D can be calculated by eq 3

$$D = \frac{l^2}{6\theta} \quad (3)$$

where θ is the time lag (s). The solution coefficient can then be derived from eq 2.

The permselectivity of a polymer film for component A relative to component B is the ratio of their permeation coefficients.

$$\alpha_{A/B} = \frac{P_A}{P_B} \quad (4)$$

Since the permeation coefficient is the product of the diffusion coefficient and solubility coefficient, the permselectivity for two gases can be expressed (eq 5) as the production of diffusion selectivity and solution selectivity.

$$\alpha_{A/B} = \frac{D_A}{D_B}\frac{S_A}{S_B} \quad (5)$$

The systematic error in the permeability measurements is mainly from the determination of the membrane thickness in the order of ±5%. In addition, the systematic error of the fast diffusivity measurements originates mainly from the time resolution of the time lag (time resolution: 0.05 s). In this study, the diffusivity systematic error is not beyond 6%. In addition, the time lag has been verified with high accuracy and small errors by Petropoulus et al.[29]

Results and Discussion

Phase Behavior via Optical Observation and Scanning Electron Microscopy (SEM). All EC/TMSG, EC/TMSD1, PTMSP/TMSG, and PTMSP/TMSD1 composite films are transparent and flawless via optical observation, indicating an excellent miscibility between the polymers (PTMSP and EC)

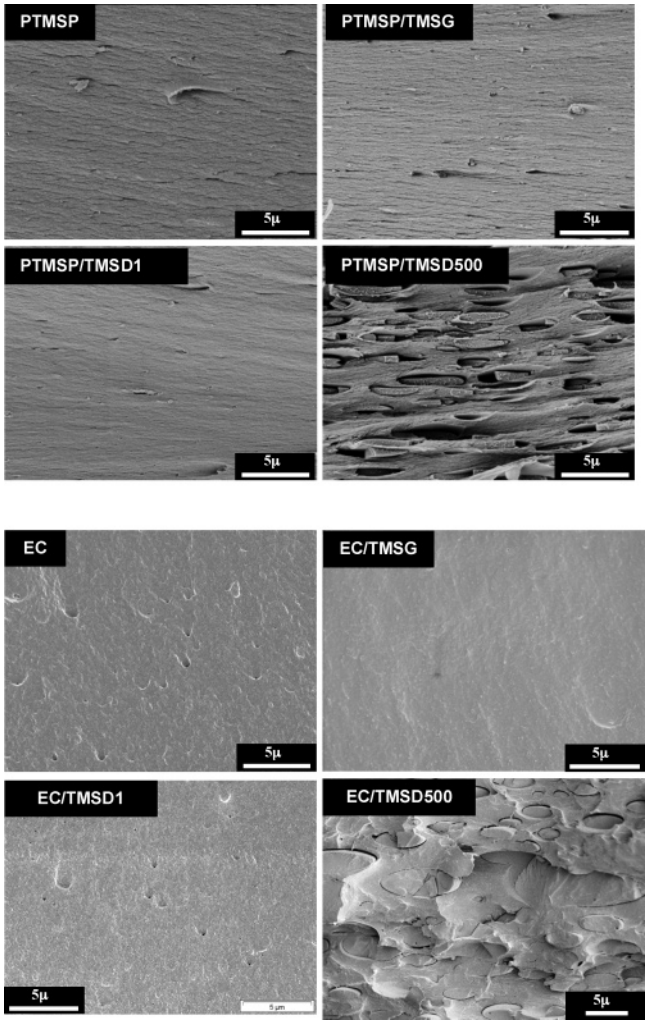

Figure 1. SEM photographies of the fracture cross section of two series of composite materials (EC/TMSS (32 vol %) and PTMSP/TMSS (27 vol %)).

and the low-M_w fillers (TMSG and TMSD1). In contrast, the EC/TMSD500 and PTMSP/TMSD500 composite films are opaque, suggesting the phase separation. The evaluation of the miscibility of composite material via the optical observation has been discussed elsewhere.[30]

Figure 1 presents SEM cross section of fractures of PTMSP and EC films containing various M_w TMSS fillers at an equivalent load content (i.e., EC/TMSS (32.1 vol %) and PTMSP/TMSS (27.2 vol %)). The homogeneous morphologies are observed in low-M_w fillers (TMSG and TMSD1) in EC and PTMSP composites. In contrast, the high-M_w TMSD500 in both polymer matrices displays heterogeneous morphologies. In the EC/TMSD500 composite, the ellipsoid TMSD500 microphase is dispersed in a continuous EC matrix. The length of the major axis for the TMSD500 ellipses varies approximately from 4 to 10 μm; the length of the minor axis varies roughly from 1 to 3.7 μm. The geometric shape factor of eccentricity for these TMSD500 ellipses in EC is nearly constant (3.1 ± 0.34). In the PTMSP/TMSD500 composite, the TMSD500 microphase forms more elongated ellipses like platelets, which distributes in a continuous PTMSP matrix similar to that observed for EC. The length of the TMSD500 microphase is in the range 3−5 μm, and its height is in the range 0.4−0.7 μm. The ratio of the length/height is nearly constant (7.5 ± 1.2). The different elongations of the filler TMSD500 in EC and PTMSP composites might be attributed to the complex interplay between

Table 3. Gas Permeabilities of the PTMSP/TMSD1 and PTMSP/TMSD500 Composite Membranes at 30 °C

composites	load (vol %)	permeability (10^{-10} cm^3 (STP) cm/ (cm^2 s cmHg))					
		He	H_2	CO_2	O_2	N_2	CH_4
PTMSP/TMSD1	9.2	2260	5307	11855	2719	1516	3753
	27.2	494	925	1695	342	128	284
	45.8	168	253	331	75	24	50
PTMSP/TMSD500	9.2	3475	8060	17450	4295	2780	7100
	27.2	1745	3816	7882	1897	1087	2858
	45.8	781	1567	2899	703	365	936

the matrix and the dispersed phase and might be also due to the different casting concentration of EC and PTMSP composite. Interestingly, a similar phase behavior was also observed for PTMSP/PPP composites investigated by Toy et al.,[23] where PPP ellipsoids were observed to disperse in a continuous PTMSP matrix via TEM.

Such phase behavior can be explained as the following. Theoretically, the phase behavior in a mixture system can be determined by the Gibbs free energy change, which combines the enthalpy change and entropy change in the mixture.[31] From the enthalpy change point of view, it seems to be reasonable to exclude the surface chemistry dissimilarity for the three saccharide-based fillers, since they have been hydrophobized with trimethylsilyl groups via the silylation with hexamethyldisilazane. Moreover, these TMSS fillers might give rise to an insignificant contribution to the combinatorial enthalpy change because the hydrophobic nature of the trimethylsilyl agent just provides a weak interaction. From the entropy change point of view, as the M_w of the TMSS filler is decreased, the combinatorial entropy change becomes more important and eventually may overcome an unfavorable combinatorial enthalpy change and lead to a homogeneous mixture.

Differential Scanning Calorimeter. At a constant content of TMSS (32.1 vol %) load in EC, a decrease of T_g in both EC/TMSG (64 °C) and EC/TMSD1 (100 °C) composite relative to that of unfilled EC (130 °C), which directly reflect increased polymer chain mobility, is observed. Moreover, the low-M_w TMSG has more impact to improve the mobility of polymer chain than a relatively high-M_w TMSD1. This difference is due to (1) TMSG has smaller size relative to TMSD1 and (2) TMSG (liquid at 30 °C) has a higher mobility than TMSD1 (solid at 30 °C). On the other side, single T_g for both of EC/TMSG and EC/TMSD1 composites further indicates a good compatibility between the polymer host and the filler, which is in good agreement with the results of the SEM and optical observation.

For the EC/TMSD500 composite, a single T_g (130 °C) appears because the glass transition temperatures of TMSD500 and EC are identical by accident (around 130 °C). In fact, the immiscible behavior for EC/TMSD500 is confirmed by SEM, which unveils that the EC chain mobility behavior is unaffected by the filler TMSD500 opposite to those in EC/TMSG and EC/TMSD1 composites.

Transport Properties of the PTMSP/TMSS System. Permeability. In Table 3, the permeabilities of six gases (He, H_2, CO_2, O_2, N_2, and CH_4) in PTMSP filled with TMSD1 and TMSD500 as a function of various load contents are illustrated. The gas transport data of the PTMSP/TMSG composites are directly obtained from our previous reports. Obviously, the incorporation of TMSS in PTMSP leads to a systematic decrease in gas permeability. In addition, the declined gas permeability seems to be related to the M_w of TMSS at a comparable load content. For instance, in PTMSP loaded with 27.2 vol % of various M_w TMSS, nitrogen permeability decreases to a large extent compared to that of unfilled PTMSP ($P(N_2) = 5490$ barrer), e.g., PTMSP/TMSG: 250-fold decrease ($P(N_2) = 22$ barrer), PTMSP/TMSD1: 43-fold decrease ($P(N_2) = 128$ barrer), and PTMSP/TMSD500: 5-fold decrease ($P(N_2) = 1087$ barrer). In order to visibly express the permeability change behavior, Figure 2 plots the normalized nitrogen permeability as a function of the loading content of various M_w TMSS. It clearly displays that the filler size is a crucial factor to affect the permeability decrease.

In PTMSP/TMSG, the drastically decreased permeability is closely related to the reduced excess large free volume in PTMSP by filled with TMSG.[20] Similarly, the considerable permeability loss in the homogeneous PTMSP/TMSD1 composite can also be explained by the same mechanism, i.e., "pore filling". However, the size of TMSD1 is difficult to be estimated because of the complex TMSD1 branch and nonspherical structure. But, the size of TMSD1 with no less than five glycoside repeat units is significantly larger than that of TMSG with a single repeat unit. Therefore, it seems to be likely that the partial TMSD1 molecule fits PTMSP micropores rather than the whole molecule, leading to the partial blockage of the FFV in PTMSP.

This assumption is indirectly supported by the fact that the permeability decreases less in PTMSP/TMSD1 than in PTMSP/TMSG at an equivalent filler load. In PTMSP/TMSG, the drastic permeability decline in PTMSP had a turning point at the loading of around 27 vol % TMSG (e.g., $P(N_2) = 22$ barrer), indirectly indicating roughly 27 vol % interconnected fractional free volume in PTMSP.[20] At equivalent load content of TMSD1 in PTMSP, the nitrogen permeability is 128 barrer. Empirically, the nitrogen permeability in most of the low FFV glassy polymers is below 50 barrer.[34−36] This value is obviously higher than that in the low FFV polymers, indicating the partially presence of the large FFV in PTMPS/TMSD1 (27 vol %). In other words, 27 vol % TMSD1 load may only partially block PTMSP micropores.

Comparatively, the drastically decreased permeability in the filled PTMSP system with different M_w PDMS fillers was also reported by Nakagawa et al.,[21] who attributed the reduced permeability to the postulated "pore filling" in PTMSP by PDMS. However, in contrast to our PTMSP/TMSS system, the high-M_w PDMS had a stronger impact on gas permeability decline in PTMSP relative to the low-M_w PDMS. It has been explained by Nakagawa et al.[21] that high-M_w PDMS just filled the large microvoids in PTMSP, but low-M_w PDMS occupied small and large microvoids in PTMSP. This difference might result from the different membrane preparation processes. The incorporation of PDMS in PTMSP was performed by an immersion process,[21] whereas we employ the polymer solution-casting process, which is described in the film preparation.

Concerning the PTMSP/TMSD500 composite, the assumption of "pore filling" seems to be not appropriate, since the size of TMSD500 (dextran500: $M_w = 350K-550K$) is apparently too large to fit into the FFV in PTMSP. In addition, the SEM reveals that TMSD500 forms micrometer size platelets dispersed in the PTMSP matrix. The gas transport in this type of heterogeneous composite can be well predicted by the modified Maxwell

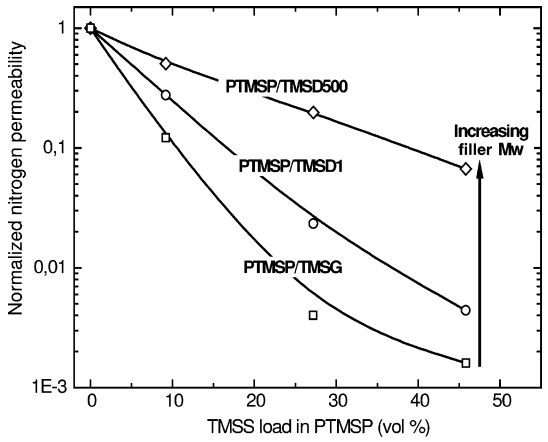

Figure 2. Normalized nitrogen permeability coefficients for PTMSP/TMSG (□), PTMSP/TMSD1 (○), and PTMSP/TMSD500 (◇) as a function of loading amount of respective TMSS filler in PTMSP.

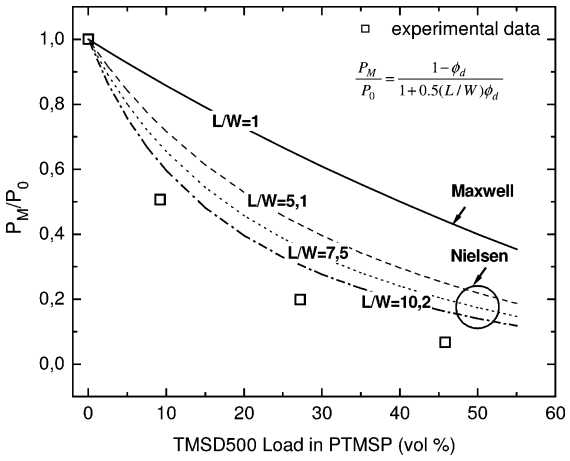

Figure 3. Normalized nitrogen permeability (P_m/P_0) (□) in PTMSP/TMSD500 as a function of TMSD500 load content in PTMSP, in comparison to that of the Maxwell model prediction[37] and Nielsen model[38] prediction with consideration of geometric factor (L/W) of dispersion phase of TMSD500 in the continuous PTMSP phase. The geometric factor $L/W = 1$ (sphere) is for the Maxwell model, and $L/W > 1$ (nonsphere) is for the Nielsen model. The geometric factors are obtained from direct measurement the dispersion phase of TMSD500 in SEM. The $L/W = 5.1$, 7.5, and 10.2 is the smallest value, average value, and largest value, respectively, from the experiment.

model,[37] which describes the gas permeability in a more permeable continuous matrix containing a dispersed, less permeable and ellipsoidal filler. Equation 6 expresses this correlation:

$$P_m = P_c\left[1 + \frac{(1 + 2W/L)\phi_d}{\frac{P_d/P_c + 2W/L}{P_d/P_c - 1} - \phi_d}\right] \quad (6)$$

where P_m, P_c, and P_d are the composite, continuous, and disperse phase permeabilities, respectively, and ϕ_d is the dispersed-phase volume fraction. Here, L and W are the length and width of the dispersed phase platelet, respectively. Because of the fragile property of TMSD500, which might result from its highly branched structure, the measurement of gas permeability for a free-standing TMSD500 film is experimentally unfeasible. However, PTMSP has the largest gas permeability known until now (at least more than 2 orders of magnitude higher than conventional, low FFV glassy polymers).[26] Therefore, it can be assumed that the dispersed TMSD500 phase is nearly

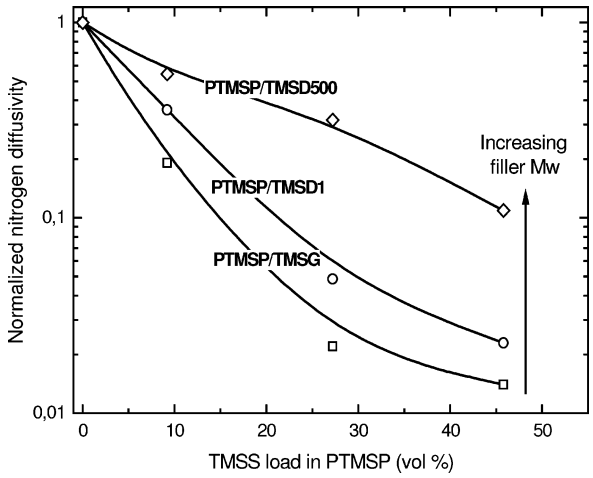

Figure 4. Normalized nitrogen diffusivity coefficients for PTMSP/TMSG (□), PTMSP/TMSD1 (○), and PTMSP/TMSD500 (◇) as a function of loading amount of respective TMSS filler in PTMSP.

Table 4. Gas Diffusivities of the PTMSP/TMSD1 and PTMSP/TMSD500 Composite Membranes at 30 °C, Which Are Derived Based on Eq 3

		diffusivity (10^{-5} cm^2/s)			
composites	load (vol %)	CO_2	O_2	N_2	CH_4
PTMSP/TMSD1	9.2	1.22	1.84	1.25	0.85
	27.2	0.23	0.34	0.17	0.10
	45.8	0.08	0.16	0.08	0.04
PTMSP/TMSD500	9.2	1.46	2.43	1.91	1.31
	27.2	1.00	1.60	1.11	0.90
	45.8	0.38	0.61	0.38	0.29

impermeable to gas compared to the PTMSP phase. Hence, eq 6 can be simplified and expressed with Nielsen's equation,[38] as described by eq 7:

$$P_m = P_c\frac{1 - \phi_d}{1 + (L/2W)\phi_d} \quad (7)$$

Figure 3 shows a favorable agreement between Nielsen's model prediction with our experimental results. The geometric factor L/W ranges from 5.1 to 10.2, which is obtained from measuring the dimension of dispersed phase TMSD500 in the continuous phase PTMSP in SEM. The average value of $L/W = 7.5$ displays slight deviation from the prediction of this model, which might be due to the uncertainty of the dimension variation of TMSD500 phase during the fractural process indicated by the SEM. Moreover, this uncertainty might be due to the negligence of permeability of TMSD500 phase in PTMSP.

In brief retrospect, the consistent tendencies in permeability decrease for various M_w TMSS fillers are observed in the PTMSP/TMSS system. In addition, the various M_w TMSS fillers result in permeability decreases to various extents. The relative size of the free volume of PTMSP and TMSS filler is crucial for the permeability decline.

Diffusivity and Solubility. Gas diffusivities (CO_2, O_2, N_2, and CH_4) in PTMSP/TMSD1 and PTMSP/TMSD500 are summarized in Table 4, which excludes He and H_2 because of their experimental uncertainties. Figure 4 plots the normalized nitrogen diffusivity as a function of loading content of various M_w TMSS. Similar to the permeability change, the consistent decrease in gas diffusivity accompanied by increased load of TMSS fillers and the decrease of filler M_w dependent diffusivity are observed. For example, at 27.2 vol % filler content in PTMSP, nitrogen diffusivity reduction is 44-fold for PTMSP/

Table 5. Gas Solubilities of the PTMSP/TMSD1 and PTMSP/TMSD500 Composite Membranes at 30 °C, Which Are Derived Based on Eq 2

composites	load (vol %)	solubility (10^{-2} cm^3 (STP)/(cm^3 cmHg)) CO_2	O_2	N_2	CH_4
PTMSP/TMSD1	9.2	9.8	1.5	1.2	4.4
	27.2	7.3	1.0	0.76	2.9
	45.8	4.0	0.48	0.31	1.3
PTMSP/TMSD500	9.2	12.0	1.8	1.5	5.4
	27.2	7.9	1.2	0.98	3.2
	45.8	7.6	1.2	0.97	3.3

TMSG (0.08×10^{-5} cm^2/s), 21-fold for PTMSP/TMSD1 (0.17×10^{-5} cm^2/s), and 3-fold for PTMSP/TMSD500 (1.11×10^{-5} cm^2/s) compared to that of unfilled PTMSP (3.5×10^{-5} cm^2/s). The drastic decrease of diffusivity PTMSP/TMSD1 composites is undoubtedly due to the "pore filling", as previously discussed. However, in PTMSP/TMSD500 (27.2 vol %), the nitrogen diffusivity is in the same order as that in PTMSP. This might be result from an increased gas diffusion path length in PTMSP by the less permeable TMSD500 dispersed phase rather than from the PTMSP FFV change.

Noticeably, the polyacetylene family exhibits a wide range of difference in diffusivity primarily due to the different polymer chain packing by the variously substituted groups.[26] It is interesting to directly compare the gas diffusivity behavior in our PTMSP/TMSS system with that in substituted polyacetylenes. Figure 5 presents the correlation between oxygen diffusivity and oxygen/nitrogen diffusivity selectivity for 19 substituted polyacetylenes (data from Masuda et al.[39]), which consist of three substituted groups (e.g., a bulky group, a long *n*-alkyl group, and a phenyl group). It can be clearly read out from Figure 5 that the behaviors of D_{O_2} and D_{O_2}/D_{N_2} in PTMSP with 27.2% and 45.8% small TMSS fillers (e.g., TMSG and TMSD1) are fairly similar to those in polyacetylenes with a long *n*-alkyl group. Compared to the bulky and rigid phenyl groups, the flexible nature of long *n*-alkyl groups may lead to an increased localized chain mobility in polyacetylenes. On the one hand, it will reduce the diffusion jump energy, resulting in increased diffusivity. On the other hand, the resultant good polymer chain packing will decrease the fractional free volume and consequently decreasing diffusivity. This phenomenon are also observed in polyacetylene with a series of different alkyl chain length by Pinnau et al.[40] Similarly, in our study, in PTMSP filled with TMSG and TMSD1 the drastically decreased FFV results in a strong gas diffusivity decrease and simultaneous diffusivity selectivity increase. On the other hand, the small and relatively mobile fillers TMSG and TMSD1 may increase the local gas diffusion to some extent but weaken the diffusivity selectivity. Regarding to the effect of localized chain mobility on gas transport properties, Singla et al.[41] have studied a series of glassy polymers. Further discussion on it is beyond the scope of this article.

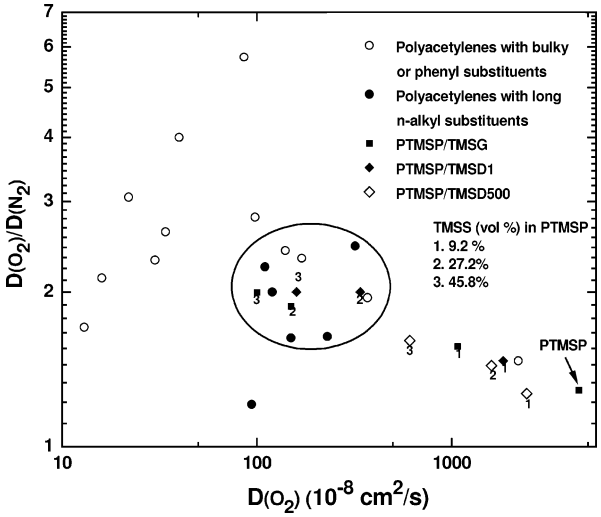

Figure 5. Relationship between oxygen diffusivity and its selectivity over nitrogen for PTMSP/TMSG (■), PTMSP/TMSD1 (◆), and PTMSP/TMSD500 (◇) composite membranes in this study. For comparison, this relationship for substituted polyacetylenes[39] with various side groups, i.e., polyacetylenes with bulky or phenyl substituents (○) and polyacetylenes with long *n*-alkyl substituents (●), are included.

The calculated gas solubility in PTMSP/TMSD1 and PTMSP/TMSD500 based on eq 2 is presented in Table 5. The increased load of different M_w TMSS in PTMSP also leads to a consistent trend of gas solubility decrease. In addition, the small size filler TMSG causes a more significant solubility reduction in PTMSP compared to the large size filler TMSD500. For example, at 27.2 vol % load of TMSS in PTMSP, the nitrogen solubility reduces by 5.4-fold for PTMSP/TMSG (0.291×10^{-2} cm^3 (STP)/(cm^3 cmHg)), 2.1-fold for PTMSP/TMSD1 (0.76×10^{-2} cm^3 (STP)/(cm^3 cmHg)), and 1.6-fold for PTMSP/TMSD500 (0.98×10^{-2} cm^3 (STP)/cm^3 cmHg) compared to the unfilled PTMSP (1.56×10^{-2} cm^3 (STP)/cm^3 cmHg). The relative diffusivity change is higher than the relative solubility change, which suggests that the diffusivity variation in PTMSP/TMSS system is mainly responsible for the permeability change.

The gas solubility in a composite system can be roughly estimated by the additive model[42] described by eq 8:

$$S_m = S_0(1 - \phi) + S_f\phi \tag{8}$$

where S_m is the solubility in the polymer composite, ϕ is the filler volume fraction, S_0 is the gas solubility in the unfilled polymer, and S_f is the gas solubility in the filler. Gas solubility

Table 6. Gas Permeabilities of the EC/TMSG, EC/TMSD1, and EC/TMSD500 Composite Membranes at 30 °C

composites	load (vol %)	permeability (10^{-10} cm^3 (STP) cm/(cm^2 s cmHg)) He	H_2	O_2	N_2	CH_4	CO_2
EC/TMSG	0.0	40.2	56.0	11.8	3.5	7.1	70.9
	11.4	51.9	72.6	16.8	4.9	10.9	94.0
	32.1	58.0	78.2	20.3	6.1	13.4	93.8
	53	79.2	113	37.3	12.3	31.0	176
EC/TMSD1	11.4	50.4	71.5	15.4	5.1	10.2	90.6
	32.1	65.8	91.9	22.1	6.3	13.6	112.7
	53	87.6	123.8	31.3	10.2	21.2	154.1
EC/TMSD500	11.4	48.8	69.2	14.5	4.8	9.1	89.7
	32.1	56.0	77.3	17.1	5.7	10.0	95.4
	41.9	79.6	111.9	27.6	8.5	17.6	147

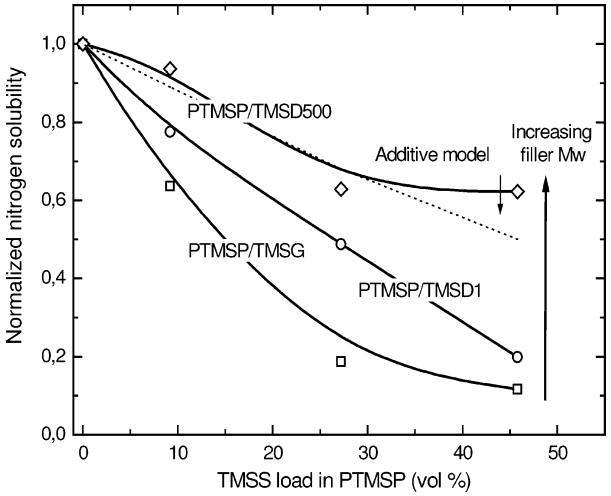

Figure 6. Normalized nitrogen solubility coefficients in PTMSP/TMSG (□), PTMSP/TMSD1 (○), and PTMSP/TMSD500 (◇) composites as a function of TMSS loading amount at 30 °C, in comparison of the additive model, as shown by a dashed line.

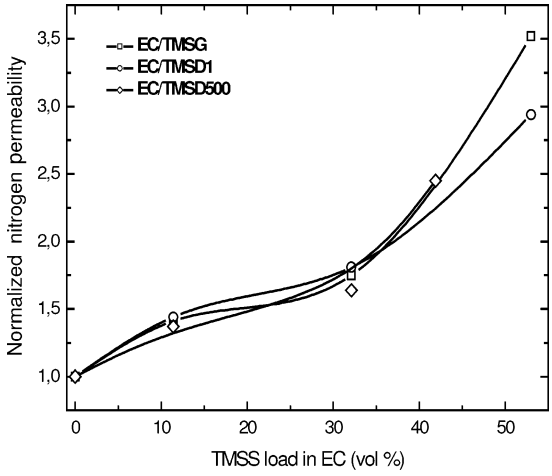

Figure 7. Normalized nitrogen permeability coefficients for EC/TMSG (□), EC/TMSD1 (○), and EC/TMSD500 (◇) as a function of loading amount of respective TMSS filler in EC.

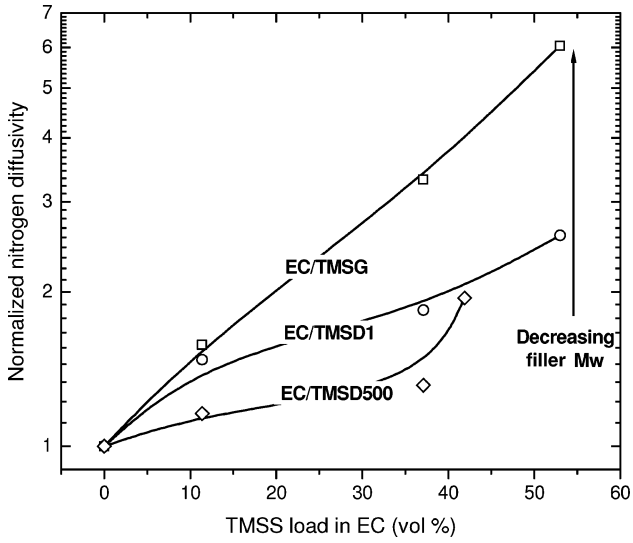

Figure 8. Normalized nitrogen diffusivity coefficients for EC/TMSG (□), EC/TMSD1 (○), and EC/TMSD500 (◇) as a function of loading amount of respective TMSS filler in EC.

in PTMSP is nearly 10 times higher than that in conventional glassy polymers, attributed to a large microporous structure for gas sorption.[26] Therefore, the gas solution in TMSS can be neglected relative to that in PTMSP. Equation 8 can be simplified as eq 9:

$$S_m = S_0(1 - \phi) \tag{9}$$

Figure 6 presents the experimentally determined nitrogen solubility in PTMSP/TMSS composites as a function of filler content, as well as the prediction of the additive model based on eq 9. It is obvious that the solubilities in both of PTMSP/TMSG and PTMSP/TMSD1 composites have a negative departure from this model. These departures might be attributed to the postulated "pore filling" in PTMSP by TMSG and TMSD1, leading to less open micropores in PTMSP for gas absorption, and a strongly reduced gas solubility which was discussed in our previous work.[20] However, the nitrogen solubility in PTMSP/TMSD500 is fairly close to the prediction of the additive model. This behavior can be reasonably explained by the fact that PTMSP intrinsic micropores are nearly intact in the PTMSP/TMSD500 composite with microscopic phase separation. Resultantly, gas solubility in this composite is just the sum of gas sorption in the two phases.

Transport Properties of EC/TMSS Composites. Permeability. In Table 6, the permeabilities of six gases (He, H_2, CO_2, O_2, N_2, and CH_4) in EC filled with various M_w TMSS are illustrated. Figure 7 plots the normalized nitrogen permeability as a function of the loading content of various M_w TMSS in EC. In contrast to the permeability decrease in the PTMSP/TMSS system, a consistent trend of permeability increase in EC/TMSS is observed. In addition, the permeability increase seems to be not well related to the filler's M_w compared to that in the PTMSP/TMSS system. For example, as EC is loaded with 32 vol % TMSG, TMSD1, and TMSD500, the increase of nitrogen permeability is fairly constant, i.e., EC/TMSG: 1.75-fold (6.1 barrer), EC/TMSD1: 1.81-fold (6.3 barrer), and PTMSP/TMSD500: 1.64-fold (5.7 barrer) compared to that in unfilled EC (3.5 barrer).

In the conventional, low FFV glassy polymer EC (FFV: 0.15), the "pore-filling" behavior cannot take place, since even the smallest filler TMSG (~1 nm) is too large to fit the FFV in EC. This is supported by the fact that the average diameter of FFV in conventional, glassy polymer is around 0.2 nm.[33] Furthermore, it seems to be implausible that both of flexible TMSS fillers disrupt EC chain packing like the rigid FS in PTMSP, where the increased FFV results in the increased permeability.

The FFV approach does not seem to be a key factor for the permeability increase in EC/TMSG and EC/TMSD1. However, the increased permeability is obviously mainly attributed to the increased polymer chain mobility, revealed by the decreased T_g accompanied by the loading of TMSG and TMSD1 in EC. In other words, TMSG and TMSD1 in EC seem to act as plasticizers, which can efficiently separate the EC chains and cause the polymer chains to more easily slip. As a result, the opportunity for gas molecular diffusion jump increases more readily in the "plasticized" chains relative to that in the rigid chain.[43] Therefore, an increased gas permeability is observed in both of the composites.

However, in EC/TMSD500, the increased gas permeability might not be a consequence of plasticization, which is indicated by the microphase separation for EC/TMSD500 with SEM. The gas transport through this type of heterogeneous medium is a result of collective transport in the EC and TMSD500 phases. The increased gas permeability in EC filled with TMSD500

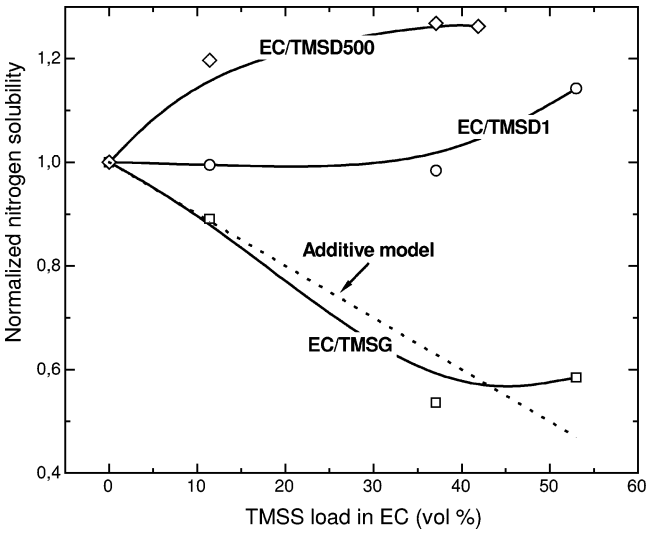

Figure 9. Normalized nitrogen solubility coefficients in EC/TMSG (□), EC/TMSD1 (○), and EC/TMSD500 (◇) composites as a function of TMSS loading amount at 30 °C, in comparison of the additive model, as shown by a dashed line.

Table 7. Gas Diffusivities of the EC/TMSG, EC/TMSD1, and EC/TMSD500 Composite Membranes at 30 °C, Which Are Derived Based on Eq 3

		diffusivity (10^{-8} cm^2/s)			
composites	load (vol %)	CO_2	O_2	N_2	CH_4
EC/TMSG	0	14	43	20	9
	11.4	24	65	30	15
	32.1	43	115	63	32
	53	86	198	115	68
EC/TMSD1	11.4	19	54	28	12
	32.1	28	78	35	18
	53	38	103	49	26
EC/TMSD500	11.4	18	48	22	11
	32.1	20	57	25	13
	41.9	30	78	37	18

can be explained by a higher permeability in the TMSD500 phase relative to that in EC phase. This speculation is based on (1) the same repeat units of TMSD500 and EC, i.e., glycoside; (2) their same backbone structure, but the highly branched TMSD500 may have a looser packing structure than a relatively linear EC, resulting in a higher FFV in TMSD500; and (3) their same backbone structure, but the side group of trimethylsilyl in TMSD500 is more flexible relative to the ethyl side group in EC, resulting in a higher, localized mobility in TMSD500 compared to that in EC.

Diffusivity. Table 7 presents the diffusion coefficients of four gases (CO_2, O_2, N_2, and CH_4) in EC/TMSS composites. Figure 8 plots the normalized nitrogen diffusivities for EC with TMSG, TMSD1, and TMSD500 as a function of their load contents. With increasing load of TMSS in EC the diffusivity increases systematically. In addition, the diffusivity increase is dependent on the M_w of TMSS in EC, in contrast to the permeability, which seems to be independent of the M_w of TMSS fillers. The diffusivity increases with decreasing M_w of TMSS. For example, at a constant 32% load of TMSS fillers, the nitrogen diffusivity increases 3.2-fold in EC/TMSG (63×10^{-8} cm^2/s), 1.7-fold in EC/TMSD1 (35×10^{-8} cm^2/s), and 1.2-fold in EC/TMSD500 (25×10^{-8} cm^2/s) compared to that of unfilled EC (20×10^{-8} cm^2/s).

The impacts on the EC chain mobility by various M_w TMSS fillers cause the corresponding changes in gas diffusivities at an equivalent filler load. The extent of gas diffusivity increase in EC/TMSS is well related to the declined T_g at 32 vol % filler load, which is ranked in the order of EC/TMSG < EC/TMSD1 < EC/TMSD500. The observed behavior can also be interpreted in terms of FFV. The FFV of filled EC polymers is usually higher than the pure EC thanks to the higher FFV of the fillers, which is inversely related to the filler molecular weight. Furthermore, the effect on EC chain mobility by a series of TMSS fillers can also be recognized from gas molecule diffusivity selectivity. It is well-known that an increase in polymer chain mobility will generally lead to a reduction in molecular diffusivity selectivity. For example, the flexible rubbery polymer PDMS has a very low diffusivity selectivity. The small molecule O_2 ($d_{eff} = 0.289$ nm) has a higher diffusivity than the relatively large CH_4 ($d_{eff} = 0.318$ nm) in the glassy polymer EC ($D(O_2)/D(CH_4) = 4.8$). At equivalent 52 vol % load of small TMSS fillers in EC, the O_2/CH_4 diffusivity selectivity reduction in EC/TMSG, EC/TMSD1, and EC/TMSD500 is about 40%, 16%, and 8%, respectively. Obviously, this diffusivity selectivity reduction is well correlated to the extent of EC chain mobility increase by various TMSS fillers. In contrast to the EC/TMSS system, the increased molecular diffusivity selectivity in PTMSP/TMSS is caused by the various extents of blockages of weak size-selective micropores in PTMSP.

Table 8. Gas Solubilities of the EC/TMSG, EC/TMSD1, and EC/TMSD500 Composite Membranes at 30 °C, Which Are Derived Based on Eq 2

		solubility (10^{-2} cm^3 (STP)/(cm^3 cmHg))			
composites	load (vol %)	CO_2	O_2	N_2	CH_4
EC/TMSG	0	4.7	0.27	0.18	0.74
	11.4	3.9	0.26	0.16	0.72
	32.1	2.2	0.17	0.10	0.43
	53	2.5	0.19	0.11	0.46
EC/TMSD1	11.4	4.9	0.28	0.18	0.83
	32.1	4.1	0.28	0.18	0.76
	53	4.0	0.31	0.21	0.83
EC/TMSD500	11.4	5.1	0.30	0.22	0.85
	32.1	4.7	0.30	0.23	0.84
	41.9	4.9	0.35	0.23	0.98

Solubility. The calculated solubility data are displayed in Table 8. Figure 9 presents the relative nitrogen solubility in EC/TMSS systems as a function of filler content. Compared to the consistent trend of the solubility decrease in PTMSP/TMSS systems, no uniform trend of solubility change in EC/TMSS is observed. In the EC/TMSG composite, the gas solubility decreases as TMSG content increases, which is quite consistent with the prediction of the additive model. However, another more plausible explanation is the decreased gas solubility in EC/TMSG attributed to a decreased "excess FFV" in EC/TMSG composite. It is generally known that a surplus in FFV (i.e., excess FFV) in glassy polymers exists owing to restricted polymer segmental mobility in the glassy state compared to rubbery polymer in an equilibrium state.[4] Therefore, gas solubility in a glassy polymer is generally somehow higher than that in rubbery polymer. As TMSG in EC acts as a plasticizer, the plasticized EC polymer chain will relax more easily, leading to a reduced "excess FFV" and consequently a reduced gas absorption. This similar behavior in EC/TMSG and PTMSP/TMSG further reveals that the "excess free volume" is a critical factor for gas absorption.

Concerning gas absorption behavior in the EC/TMSD1 composite, the nitrogen solubility is constant in EC filled with a small portion of TMSD1 (11 and 32 vol %). With a further increased content of TMSD1, the solubility increases slightly by about 10%. The filler TMSD1 plasticizes the EC polymer

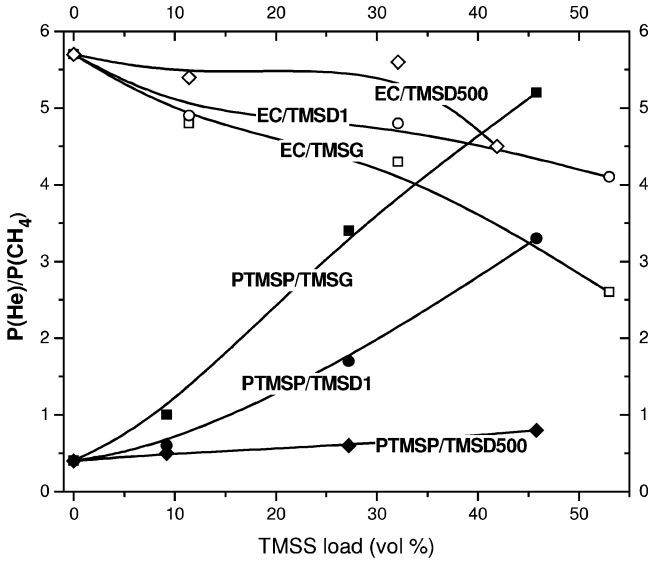

Figure 10. Selectivity of He/CH_4 in EC/TMSG (□), EC/TMSD1 (○), EC/TMSD500 (◇), PTMSP/TMSG (■), PTMSP/TMSD1 (●), and PTMSP/TMSD500 (◆) composites as a function of loading amount of respective TMSS filler.

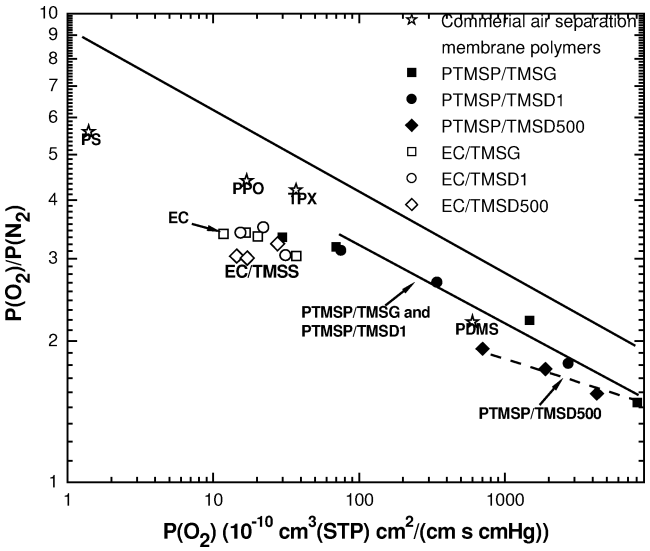

Figure 11. Relationship between oxygen permeability and its selectivity over nitrogen for EC/TMSG (□), EC/TMSD1 (○), EC/TMSD500 (◇), PTMSP/TMSG (■), PTMSP/TMSD1 (●), and PTMSP/TMSD500 (◆) composite membranes in this study. For comparison, this relationship for several commercial air separation membranes[44] (e.g., poly(dimethylsiloxane) [PDMS], poly(4-methyl-1-pentene) [TPX], poly(2,6-dimethylphenylene oxide) [PPO], and polysulfone [PS]). The upper bound line comes from Robeson.[15]

chain less than TMSG, indicated by the T_g comparisons. Resultantly, the reduced "excess FFV" in EC by TMSD1 is less than that in EC/TMSG. In addition, compared to the rubberlike TMSG, a glassy oligomer TMSD1 might introduce extra "excess FFV" in this composite at 30 °C, which will more or less compensate the reduced "excess FFV" caused by the plasticization effect.

In the EC/TMSD500 composite, an increased gas solubility is observed with the increased load of TMSD500. Contrary to the impact on the "excess FFV" in EC by low-M_w analogies TMSG and TMSD1, the solubility change in EC/TMSD500 might be just the sum of the solubilities in both EC and TMSD500 phases, which is similar to that in PTMSP/TMSD500 composites. Since the microsized phase separation in EC/TMSD500 and PTMSP/TMSD500 is revealed by SEM, the increased gas solubility for this composite might be due to the fact that TMSD500 has a higher gas sorption than EC.

Permselectivity. He/CH_4 Permselectivity in the PTMSP/TMSS and EC/TMSS Systems. The unusual, large FFV in PTMSP causes a weaker gas-size-dependent selectivity compared to conventional, low FFV polymers.[26] For example, the permeability of the small gas He ($d_{eff} = 0.178$ nm) is even 2.5-fold lower than that of the large gas CH_4 ($d_{eff} = 0.318$ nm) in PTMSP. In contrast, in the low FFV, glassy polymer ethylcellulose, the P(He) is 5.7-fold faster than the $P(CH_4)$. The permeability change as a function of gas diameter is extraordinarily sensitive to polymer FFV and chain mobility change. In order to clearly visualize the impacts of the free volume change in PTMSP and the chain mobility variation in EC on the gas size-selectivity behavior by the loading of various M_w TMSS fillers, Figure 10 plots the He/CH_4 selectivity as a function of loading content of TMSG, TMSD1, and TMSD500 in PTMSP and EC. The high-M_w filler TMSD500 in PTMSP and EC insignificantly alters the He/CH_4 selectivity, which is in good agreement with the observation of phase separation by SEM. Therefore, nearly undisturbed FFV in the continuous PTMSP phase and almost unchanged chain mobility in the continuous EC phase are the result. Additionally, the lowest M_w filler TMSG in both systems has the strongest influence on the variation of the He/CH_4 selectivity compared to higher M_w TMSS fillers at the equivalent filler load. In the opposite way, the He/CH_4 selectivity systematically increases in PTMSP with increasing load of TMSG and TMSD1, which serves as another indirect evidence of the "pore filling".

O_2/N_2 Permselectivity in PTMSP/TMSS and EC/TMSS Systems. It is worthwhile to review the oxygen/nitrogen separation in PTMSP/TMSS and EC/TMSS systems, since air separation is the largest market in gas separation. In Figure 11, the O_2/N_2 selectivity and O_2 permeability for PTMSP/TMSS and EC/TMSS composites are presented. Four commercial air separation membrane materials[44] (PDMS, poly(4-methyl-1-pentene) (TPX), poly(2,6-dimethyl-1,4-phenylene oxide) (PPO), and polysulfone (PS)) are also included, in addition to the well-known Robeson's upper bond.[15] The PTMSP/TMSD1 composites also shows a similar O_2/N_2 separation performance relative to PTMSP/TSMG. However, in PTMSP/TMSD500, the decreased permeability cannot be sufficiently compensated by the increased selectivity compared to those in other two analogue composites. Compared to the fastest permeability polymer PDMS, the transport properties in PTMSP/TMSG and PTMSP/TMSD1 is noticeably located more close to the Robeson's upper bond.

Ethylcellulose was one of the first successful polymers for commercial air separation membranes.[44,45] The addition of TMSS fillers into EC leads to a significant permeability increase with only a slight selectivity loss. With a permeability of 50 barrer and an O_2/N_2 selectivity of more than 3, the EC/TMSS composite might be as an attractive low cost material for oxygen enrichment.

Summary

In the rigid, high free volume PTMSP filled with TMSS, gas permeability, diffusivity, and solubility decreased consistently with increasing filler content. Low-M_w fillers (e.g., TMSG and TMSD1) led to a stronger reduction of gas transport parameters compared to the high-M_w filler TMSD500. The small fillers caused a reduction of the free volume. Consequently, permeability, diffusivity, and solubility were reduced. The large filler TMSD500, on the other hand, was too large to occupy the free

volume elements of PTMSP. A microsized phase separation could be observed by SEM. In this composite, the reduced permeability could be attributed to the combined permeability in both PTMSP and TMSD500 phases.

Contrary to the PTMSP/TMSS system, the TMSS filled EC (low FFV) showed a higher gas permeability than the pure polymer. Additionally, no clear correlation between M_w of the filler and permeability increase could be observed. The low-M_w fillers TMSG and TMSD1 led to a decreased T_g and an increase of gas diffusivity, which can be explained by an increase in chain mobility (plasticization effect). Moreover, the plasticization simultaneously leads to a reduction of "excess FFV" in the glassy polymer EC, resulting in a decrease of gas sorption. Similar to the PTMSP/TMSD500 composite, the high-M_w filler TMSD500 did not change the polymer chain mobility and the FFV, which is also supported by SEM observation and T_g measurements. The increased permeability, diffusivity, and sorption can be explained by the combination of the transport properties of the EC and TMSD500 phases.

Acknowledgment. The authors thank Marion Aderhold and Michael Schossig for help with the SEM work, Maren Eggers for DSC and TGA measurements, and Sergey Shishatskiy for the determination of the time-lag resolution. Part of this work was supported by the European Commission (Project COMPOSE, project no. NMP-CT-2003-505633-1). J.-M. Zheng is grateful to the Portuguese Foundation for Science and Technology (FCT) for the postdoctoral grant (reference: SFRH/BPD/14489/2003).

References and Notes

(1) Wijmans, J. G.; Baker, R. W. *J. Membr. Sci.* **1995**, *107*, 1.
(2) Petropoulos, J. H. *J. Membr. Sci.* **1990**, *53*, 229.
(3) Petropoulos, J. H. *Membr. Proc. Indo-EC Workshop* **1991**, 253.
(4) Van Krevelen, D. W. *Properties of Polymers*, 3rd completely revised ed.; Elsevier: Amsterdam, 1997.
(5) Alentiev, A. Y.; Shantarovich, V. P.; Merkel, T. C.; Bondar, V. I.; Freeman, B. D.; Yampolskii, Y. P. *Macromolecules* **2002**, *35*, 9513.
(6) Cohen, M. H.; Turnbull, D. *J. Chem. Phys.* **1959**, *31*, 1164.
(7) Jia, L.; Xu, J. *Polymer* **1991**, *23*, 417.
(8) Thran, A.; Kroll, G.; Faupel, F. *J. Polym. Sci., Part B: Polym. Phys.* **1999**, *37*, 3344.
(9) Nagel, C.; Gunther-Schade, K.; Fritsch, D.; Strunskus, T.; Faupel, F. *Macromolecules* **2002**, *35*, 2071.
(10) Srinivasan, R.; Auvil, S. R.; Burban, P. M. *J. Membr. Sci.* **1994**, *86*, 67.
(11) Pinnau, I.; Toy, L. G. *J. Membr. Sci.* **1996**, *116*, 199.
(12) Stern, S. A. *J. Membr. Sci.* **1994**, *94*, 1.
(13) Budd, P. M.; Msayib, K. J.; Tattershall, C. E.; Ghanem, B. S.; Reynolds, K. J.; McKeown, N. B.; Fritsch, D. *J. Membr. Sci.* **2005**, *251*, 263.
(14) Freeman, B. D. *Macromolecules* **1999**, *32*, 375.
(15) Robeson, L. *J. Membr. Sci.* **1991**, *62*, 165.
(16) Lin, H.; van Wagner, E.; Freeman, B. D.; Toy, L. G.; Gupta, R. P. *Science* **2006**, *311*, 639.
(17) Merkel, T. C.; Freeman, B. D.; Spontak, R. J.; He, Z.; Pinnau, I.; Meakin, P.; Hill, A. J. *Science* **2002**, *296*, 519.
(18) Higuchi, A.; Yoshida, T.; Imizu, T.; Mizoguchi, K.; He, Z.; Pinnau, I.; Nagai, K.; Freeman, B. D. *J. Polym. Sci., Part B: Polym. Phys.* **2000**, *38*, 1749.
(19) Langsam, M.; Puri, P. S.; Anand, M.; Laciak, D. V. U.S. Patent 4,-859,215, Aug 22, 1989 (Air Products and Chemicals, Inc.).
(20) Qiu, J.; Zheng, J.-M.; Peinemann, K.-V. *Macromolecules* **2006**, *39*, 4093.
(21) Nakagawa, T.; Fujisaki, S.; Nakano, H.; Higuchi, A. *J. Membr. Sci.* **1994**, *94*, 183.
(22) Nagai, K.; Kanehashi, S.; Tabei, S.; Nakagawa, T. *J. Membr. Sci.* **2005**, *251*, 101.
(23) Toy, L. G.; Freeman, B. D.; Spontak, R. J.; Morisato, A.; Pinnau, I. *Macromolecules* **1997**, *30*, 4766.
(24) Andrady, A. L.; Merkel, T. C.; Toy, L. G. *Macromolecules* **2004**, *37*, 4329.
(25) Tantekin-Ersolmaz, S. B.; Atalay-Oral, C.; Tatlier, M.; Erdem-Senatalar, A.; Schoeman, B.; Sterte, J. *J. Membr. Sci.* **2000**, *175*, 285.
(26) Nagai, K.; Masuda, T.; Nakagawa, T.; Freeman, B. D.; Pinnau, I. *Prog. Polym. Sci.* **2001**, *26*, 721.
(27) Schossig-Tiedemann, M. *Beitr. Elektronenmikroskop. Direktabb. Oberfl.* **1994**, *27*, 209.
(28) Shishatskii, S.; Yampol'skii, Yu. P.; Peinemann, K.-V. *J. Membr. Sci.* **1996**, *112*, 275.
(29) Petropoulos, J. H.; Myrat, C. *J. Membr. Sci.* **1977**, *2*, 3.
(30) Roberto, A. K. Transmission and reflection of light in multiphase media. In *Polymer Blends: Formulation and Performance*; Paul, D. R., Bucknall, C. B., Eds.; John Wiley & Sons: New York, 2000; pp 301−304.
(31) Merfeld, G. D.; Paul, D. R. *Polymer-Polymer Interactions Based on Mean Field Approximations*; Paul, D. R., Bucknall, C. B., Eds.; John Wiley & Sons: New York, 2000; pp 55−91.
(32) Shantarovich, V. P.; Kevdina, I. B.; Yampolskii, Yu. P.; Alentiev, A. Yu *Macromolecules* **2000**, *33*, 7453.
(33) Hofmann, D.; Heuchel, M.; Yampolskii, Y.; Khotimskii, V.; Shantarovich, V. *Macromolecules* **2002**, *35*, 2129.
(34) Hwang, S. T.; Choi, C. K.; Kammermeyer, K. *Sep. Sci.* **1974**, *9*, 461.
(35) Pauly, S. Permeability and diffusion data. In *Polymer Handbook*, 4th ed.; Brandrup, J., Immergut, E. H., Grulke, E. A., Eds.; John Wiley & Sons: New York, 1999; VI/543−VI/569.
(36) Park, J. Y.; Paul, D. R. *J. Membr. Sci.* **1997**, *125*, 23.
(37) Petropoulos, J. H. Membrane with non-homogenous sorption and transport properties. In *Polymer Membranes*; Gordon, M.; Ed.; Springer-Verlag: Berlin, 1985; pp 93−142.
(38) Nielsen, L. E. *J. Macromol. Sci., Chem.* **1967**, *A1*, 929.
(39) Masuda, T.; Iguchi, Y.; Tang, B.-Z.; Higashimura, T. *Polymer* **1988**, *29*, 2041.
(40) Pinnau, I.; Morisato, A.; He, Z. *Macromolecules* **2004**, *37*, 2823.
(41) Singla, S.; Beckham, H. W.; Rezac, M. E. *J. Membr. Sci.* **2002**, *208*, 257.
(42) Merkel, T. C.; Freeman, B. D.; Spontak, R. J.; He, Z.; Pinnau, I.; Meakin, P.; Hill, A. J. *Chem. Mater.* **2003**, *15*, 109.
(43) Crank, J.; Park, G. S. *Diffusion in Polymers*; Academic: London, 1986.
(44) Nunes, S.-P.; Peinemann, K.-V. Gas separation with membranes. In *Membrane Technology in the Chemical Industry*; Nunes, S.-P., Peinemann, K.-V., Eds.; Wiley-VCH: Weinheim, 2001; pp 39−67.
(45) Baker, R. W. *Ind. Eng. Chem. Res.* **2002**, *41*, 1393.

MA0614794